

# Morphology of Protonated Methanol Clusters: An Infrared Spectroscopic Study of Hydrogen Bond Networks of $\text{H}^+(\text{CH}_3\text{OH})_n$ ( $n = 4-15$ )

Asuka Fujii,\* Satoko Enomoto, Mitsuhiro Miyazaki,<sup>†</sup> and Naohiko Mikami\*

Department of Chemistry, Graduate School of Science, Tohoku University, Sendai 980-8578, Japan

Received: August 13, 2004; In Final Form: October 24, 2004

Infrared spectroscopy of large-sized protonated methanol clusters,  $\text{H}^+(\text{MeOH})_n$  ( $n = 4-15$ ), was carried out in the OH stretch region to characterize the development of the hydrogen bond network with the cluster size,  $n$ . The band intensity of the free OH stretching mode decreased with  $n$ , and the band finally disappeared at  $n = 7$ . On the other hand, the broad absorption band due to hydrogen-bonded OH stretches exhibited a remarkable shift with the cluster size, and it finally converged on  $3300 \text{ cm}^{-1}$  for  $n \geq \sim 10$ . The size dependence of the infrared spectra was morphologically interpreted in terms of the formation of the bicyclic hydrogen-bonded structure of the clusters.

## Introduction

The hydrogen bond has been one of the most important chemical subjects, and great efforts have been dedicated to elucidate its nature.<sup>1</sup> To establish a microscopic picture of the hydrogen bond is an ultimate goal of gas-phase spectroscopy of molecular clusters, and significant progress has been achieved in the past decade by application of infrared (IR) spectroscopy to size-selected clusters in combination with the development of quantum chemical calculations.<sup>2-6</sup> Very recently, such an approach has been applied to large-sized protonated water clusters,  $\text{H}^+(\text{H}_2\text{O})_n$ , up to  $n = 27$ .<sup>7-9</sup> IR spectroscopy of the OH stretch region successfully clarified the stepwise development of the hydrogen bond network with size; the chain-type structures are transformed to net-type structures, and then the three-dimensional (3-D) cage structure is completed at  $n = 21$ ,<sup>7-9</sup> which is the well-known magic number in the cluster size distribution of the mass spectrum.<sup>10,11</sup> This result well reveals how the tetrahedral coordination nature of water induces the 3-D structure of hydrogen bond network in protonated water. Moreover, these studies clearly demonstrated the utility of IR spectroscopy for structural analysis of large-sized clusters including more than 10 molecules.<sup>7-9,12</sup>

In contrast to such extensive studies on the hydrogen bond nature of water clusters, studies on the hydrogen bond of methanol clusters have been much less extensive,<sup>13-19</sup> though methanol is a prototype to understand hydrogen bonds in alcohols. While water can be four-coordinated and the double-proton-donating site plays a very important role to form the 3-D hydrogen-bonded structures, methanol can be three-coordinated at maximum and no double-proton donation is allowed. Such a difference in the hydrogen bond nature would cause a type of hydrogen bond network of methanol totally different from that of water. An X-ray diffraction study suggested that methanol basically forms chainlike structures in the liquid phase.<sup>20</sup> On the other hand, IR spectroscopy of neutral methanol clusters,  $(\text{MeOH})_n$  ( $n = 2-9$ ), in the gas phase

demonstrated that the clusters of  $n = 3$  to  $n = 9$  have cyclic structures to maximize the number of hydrogen bonds in the system.<sup>13-17</sup> A mixed cluster system, benzene- $(\text{MeOH})_n$  ( $n = 1-6$ ), was also studied by IR spectroscopy, and it was shown that the methanol moiety still holds the cyclic structures though the hydrogen-bonded ring is distorted for  $n > 3$  to solvate the aromatic ring.<sup>18,19</sup>

As for the protonated methanol,  $\text{H}^+(\text{MeOH})_n$ , experimental information on the hydrogen bond structure is very limited,<sup>21-23</sup> despite its importance as a model of the proton solvation by molecules other than water. Chang et al. carried out IR spectroscopy of the clusters of  $n = 4$  and  $5$ .<sup>21,22</sup> While a linear chain structure was predominant for  $n = 4$ , the coexistence of the linear chain and the cyclic form was found for  $n = 5$ . They suggested that the interconversion between the linear and cyclic forms causes a fast intracluster proton transfer. No structural information has been available for larger protonated methanol clusters so far. Mass spectrometry of protonated methanol was performed by Zhang et al. up to  $n = 24$ ,<sup>23</sup> but no magic number, which suggests a specific structure, was found, in contrast with the case of the protonated water clusters.<sup>10,11</sup>

As was demonstrated in the previous IR studies of protonated water, IR spectroscopy of size-selected clusters enables us to probe trends of the hydrogen bond network development even in large-sized clusters.<sup>7-9</sup> In the present study, we apply IR spectroscopy to size-selected  $\text{H}^+(\text{MeOH})_n$  from  $n = 4$  up to  $n = 15$  in the OH stretch region. The IR spectra show a remarkable size dependence originating from the development of the hydrogen bond network. "Morphological" consideration of the coordination nature of methanol predicts the formation of bicyclic structures, which are qualitatively consistent with the observed IR spectra.

## Experiment

IR spectra of the  $\text{H}^+(\text{MeOH})_n$  cluster cations were recorded by IR predissociation spectroscopy using a mass spectrometer equipped with linearly aligned tandem quadrupole mass filters connected by an octopole ion guide. The details of the apparatus have already been described in previous papers,<sup>7,24</sup> and only a brief description is given here.  $\text{H}^+(\text{MeOH})_n$  was produced by a

\* To whom correspondence should be addressed. E-mail: asuka@qclhp.chem.tohoku.ac.jp (A.F.); nmikami@qclhp.chem.tohoku.ac.jp (N.M.).

<sup>†</sup> Present address: Department of Chemistry, Graduate School of Science, Kyoto University, Kyoto 606-8502, Japan.

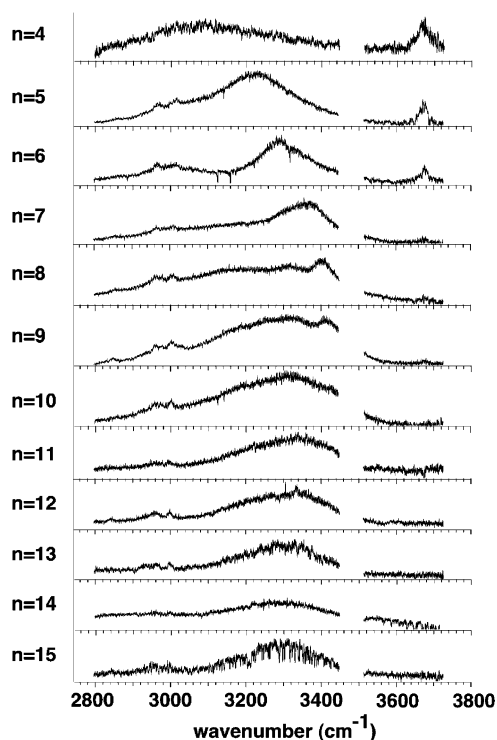


**Figure 1.** IR dissociation spectra of protonated methanol clusters,  $\text{H}^+(\text{MeOH})_n$  ( $n = 4-15$ ), in the OH stretch region. The spectra of  $n = 4-10$  and  $n = 11-15$  were measured by monitoring the  $n - 1$  and  $n - 2$  fragment cations, respectively (see the text). The spectral gap between  $3440$  and  $3520 \text{ cm}^{-1}$  was caused by the depletion of the IR laser power due to the absorption by the water impurities in the nonlinear optical crystal to generate IR light.

photoassisted discharge of methanol vapor seeded in Ne (total pressure of 3 atm). The gaseous mixture was expanded from a pulsed supersonic valve through a channel nozzle. The channel was equipped with a wire electrode at its sidewall, and a dc voltage of  $-300 \text{ V}$  relative to the channel was applied to the electrode. The discharge in the channel was triggered by irradiation of the electrode surface with a laser pulse ( $355 \text{ nm}$ ,  $5 \text{ mJ/pulse}$ ), which is synchronized with the pulsed valve operation. The  $\text{H}^+(\text{MeOH})_n$  cluster cations were cooled through the expansion from the channel. The cluster cations were size-selected by the first quadrupole mass filter and then introduced into the octopole ion guide. The mass resolution of the first mass filter was set to be higher than  $1 \text{ amu}$  to exclude the contamination of undesired cluster species. Within the octopole ion guide, the mass-selected cations were irradiated by a counterpropagating IR laser, and were sent to the second quadrupole mass filter, which was tuned to the mass of the  $n - 1$  or  $n - 2$  fragment ion produced by the vibrational excitation. Thus, an IR spectrum of the size-selected cluster was recorded by measuring the fragment ion intensity while scanning the IR laser frequency. The IR light was generated by difference frequency mixing (DFG) between the fundamental outputs of a YAG laser and a dye laser.

## Results and Discussion

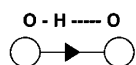
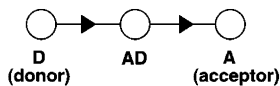
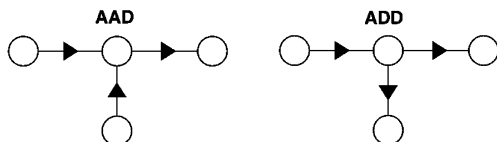
Figure 1 shows the IR dissociation spectra of  $\text{H}^+(\text{MeOH})_n$  ( $n = 4-15$ ) in the OH stretch region. The spectra of  $n = 4-10$  were measured by monitoring the  $n - 1$  fragment cations. We observed that 3–10% of the parent cluster cations spontaneously dissociate after passing through the first quadrupole mass filter. Such a spontaneously produced fragment causes a background signal in the measurement of IR spectra, and its interference

significantly reduces the quality of the spectra in the sizes of  $n > 10$ . Because the evaporation of one methanol molecule is predominant in the spontaneous dissociation paths, we observed the IR spectra of  $n = 11-15$  by monitoring the  $n - 2$  fragment to avoid the interference due to the background signal. In the size range of  $n = 11-14$ , we also measured the IR spectra by monitoring both the fragments, and we confirmed that no spectral changes occur depending on the monitoring fragmentation channel except for the quality of the spectra, as shown in the Supporting Information. All the IR spectra in Figure 1 were normalized to the laser power. The spectral gap between  $3440$  and  $3520 \text{ cm}^{-1}$  was caused by the depletion of the IR laser power due to the absorption by the water impurities in the DFG crystal.

The observed IR spectra of  $n = 4$  and  $5$  are essentially the same as those reported by Chang et al.<sup>21,22</sup> They demonstrated that the IR spectral feature of  $n = 4$  and  $5$  shows a temperature dependence, which indicates the presence of the cyclic and linear chain isomers. The present IR spectra are similar to those measured under the higher internal temperature condition of Chang et al., and both of the isomers may contribute to the spectra. Despite the contribution of several isomers, the present IR spectra show a remarkable change of the spectral features with an increase of the cluster size. Such a change represents the trend of the development of the hydrogen bond network structure.

In the spectra, the relatively sharp feature at  $3670 \text{ cm}^{-1}$  is assigned to the free OH stretching vibration, and the broad absorption in the range of  $2800-3600 \text{ cm}^{-1}$  is attributed to the hydrogen-bonded OH stretches.<sup>13,18,21,22</sup> Small shoulders seen around  $3000 \text{ cm}^{-1}$  are due to the CH stretches of the methyl group,<sup>25</sup> and the CH bands show no remarkable changes with the cluster size. The free OH stretch band becomes weaker with an increase of the cluster size, and it finally disappears at  $n = 7$ . This disappearance of the free OH stretch clearly demonstrates that the clusters form a kind of cyclic structure for  $n \geq 7$ , where all the hydroxyl groups are hydrogen-bonded with each other. Though a trace of the free OH band is actually seen for  $7 \leq n \leq 9$ , it would be the contribution of minor isomers of higher internal energies. On the other hand, though the hydrogen-bonded OH stretch bands show substantial size dependence from  $n = 4$  to  $n = 9$ , they finally converge on a broad absorption centered at  $3300 \text{ cm}^{-1}$  for  $n \geq \sim 10$ . It is worth noting that this spectral feature for  $n \geq \sim 10$  is very similar to those of cyclic neutral methanol clusters.<sup>15-19</sup>

Prior to consideration of implications in the observed IR spectra of  $\text{H}^+(\text{MeOH})_n$ , we examine the general geometrical nature of the hydrogen bond in methanol. Here we introduce schematic symbols to represent hydrogen bonds and their coordination types, as shown in Figure 2. Figure 2a represents the definition of the symbol of a hydrogen bond, where an open circle means an oxygen atom of methanol and a hydrogen bond is represented by an arrow from a proton donor to an acceptor. According to the coordination number, molecules in a hydrogen bond network are categorized into several types. In a linear hydrogen bond chain, as seen in Figure 2b, three different types of molecules exist; each terminal molecule plays a role only of a proton donor or of an acceptor, and we call such a molecule D or A, respectively. The A site molecule still has a free OH group and can donate its proton to form a new hydrogen bond. A molecule between the A and D sites is not only a proton donor but also an acceptor, and such a molecule is called AD (acceptor-donor). When a terminal molecule is bound to an AD site in a chain, branching of the hydrogen bond chain occurs,

**(a) Hydrogen bond and its direction****(b) 1- and 2-coordinated sites****(c) 3-coordinated sites**

**Figure 2.** Symbolic representations of the hydrogen bond: (a) definition of the symbol, (b) one- and two-coordinated sites in a hydrogen bond network, (c) three-coordinated sites in a hydrogen bond network.

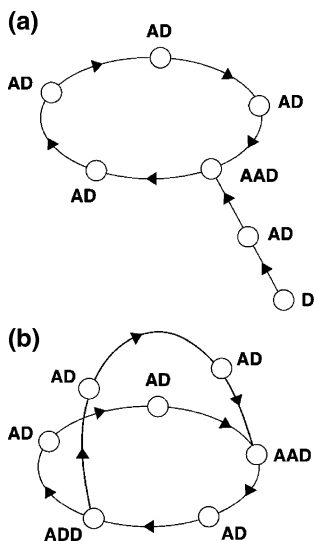


**Figure 3.** Schematic representations of hydrogen bond network structures: (a) cyclic structure in methanol clusters, (b) net-type structure formed in water clusters.

and the branching site becomes a three-coordinated site. As shown in Figure 2c, there are two types of three-coordinated sites; one is a double-acceptor single-donor (AAD) type, and the other is a single-acceptor double-donor (ADD) type. Here we should note that methanol cannot be an ADD site while water can be both of them. This difference causes a remarkable difference in the cluster structures of water and methanol.

We first examine possible hydrogen bond network structures of neutral methanol clusters,  $(\text{MeOH})_n$ . It is obvious that a linear chain and a cyclic form can be available for methanol clusters. In fact, IR spectroscopy of  $(\text{MeOH})_n$  has demonstrated that  $(\text{MeOH})_n$  forms simple cyclic structures in the size range of  $3 \leq n \leq 9$ .<sup>13–19</sup> When a branching of the ring occurs to develop into a more complicated network, the branching site should be AAD; thus, the terminal of the side chain becomes a D site, as schematically shown in Figure 3a. Because this side chain is terminated by the D site, it cannot be bound to an AD site in the ring to form another ring. Therefore, the hydrogen bond network of  $(\text{MeOH})_n$  is restricted to a chain form or a ring form with side chains. Net-type hydrogen bond structures, which are schematically shown in Figure 3b, are never formed in neutral

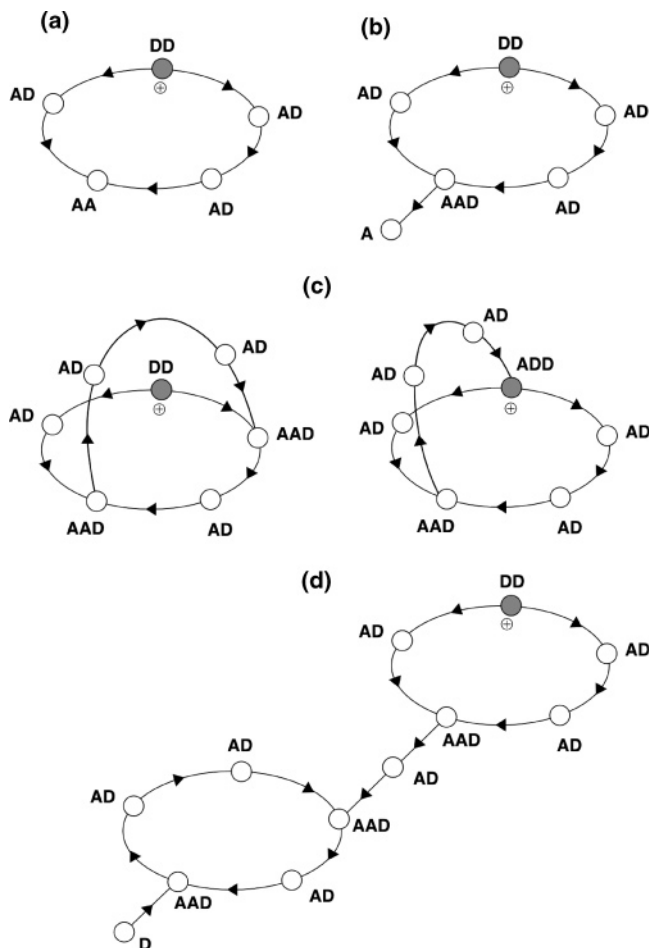


**Figure 4.** Schematic representation of hydrogen bond network development in protonated methanol clusters: (a) cyclic structure ( $n \geq 5$ ), (b) cyclic structure with a side chain ( $n \geq 6$ ), (c) bicyclic structures ( $n \geq 7$ ), (d) variation of bicyclic structures ( $n \geq 8$ ).

methanol clusters because such structures require both AAD and ADD sites.

On the other hand, in  $\text{H}^+(\text{MeOH})_n$ , the  $\text{CH}_3\text{OH}_2^+$  (or  $(\text{CH}_3\text{OH})-\text{H}^+-\text{H}^+(\text{CH}_3\text{OH})$ ) ion core can be a unique double donor (DD) site, and it partly loosens the structural restriction seen in  $(\text{MeOH})_n$ . The IR and ab initio study of  $\text{H}^+(\text{MeOH})_n$  by Chang et al. has demonstrated that the protonated methanol clusters prefer linear chain structures at  $n \leq 4$  and start to form a cyclic structure at  $n = 5$ .<sup>21,22</sup> In the cyclic structure of  $\text{H}^+(\text{MeOH})_n$ , because of the double-donor nature of the protonated site, there exists a free OH due to a double-acceptor (AA) site, as shown in Figure 4a. A linear chain can originate from this AA site with the transformation of the AA site to the AAD site (Figure 4b). Different from the case of  $(\text{MeOH})_n$ , this side chain should be terminated by an A site, and it can be bound to an AD (or to the DD) site of the ring moiety, when the chain length is long enough to form the second ring. When the free OH of the chain (terminal A site) is bound to the AD (or DD) site of the ring, a bicyclic structure is created with the transformation of the A and AD (or DD) sites to the AD and AAD (or ADD) sites, respectively. This situation is schematically represented in Figure 4c. Such a bicyclic structure formation is not allowed in  $(\text{MeOH})_n$ , but the double-donor nature of the protonated core enables  $\text{H}^+(\text{MeOH})_n$  to evolve into this more complicated structure.

The formation of the bicyclic structure is accompanied by the disappearance of the free OH. The free OH band in the IR spectra of  $\text{H}^+(\text{MeOH})_n$  is found to disappear at  $n = 7$ , and this

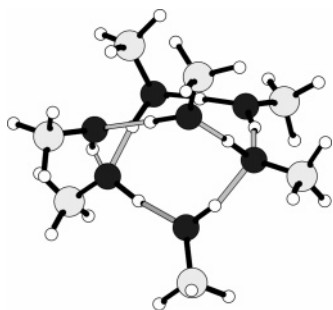


**Figure 5.** A stable [2.2.1] bicyclic structure of  $\text{H}^+(\text{MeOH})_7$  obtained by B3LYP/6-31G calculations.

is an indication that the bicyclic structure formation is completed at this size. The minimum size to form the first ring including the protonated core is  $n = 5$ ,<sup>21,22</sup> and a need of two more methanol molecules to bridge a five-membered hydrogen-bonded ring seems to be quite reasonable. We tentatively carried out density functional theory calculations at the B3LYP/6-31G level to confirm the bicyclic structure formation at  $n = 7$ ,<sup>26</sup> and a [2.2.1] bicyclic structure with the  $(\text{CH}_3\text{OH})-\text{H}^+-\text{H}^+-\text{H}^+-\text{OH}$  ion core was found as a stable structure. Its schematic structure is shown in Figure 5.<sup>27</sup> Though there might be other isomers for  $n = 7$ , this calculation result qualitatively supports the above discussion.

When the terminal methanol in the side chain is bound to the chain moiety itself, it results in an alternative bicyclic structure, as schematically shown in Figure 4d. To form the second ring in this way, the side chain should involve more than two methanol molecules, while the formation of the first ring including the ion core requires at least five molecules. Therefore, in the clusters of  $n \geq 8$ , such a variation of the bicyclic structure would be allowed.

Once these bicyclic structures are formed, more complicated net or cage formation is forbidden in  $\text{H}^+(\text{MeOH})_n$ , except for the occurrence of linear side chains from the cyclic moieties. We should note again that such a side chain cannot form another ring because it is terminated with a D site. Therefore, an increase of the cluster size would mainly result in the expansion of the sizes of the two rings. The bicyclic structures consist of AD sites except for the unique protonated core (the DD site) and two bridging AAD sites. With an increase of the ring size, the ratio of the AD sites becomes dominant. Neutral methanol clusters of the single cyclic forms consist only of AD sites, and their hydrogen-bonded OH stretches appear around  $3300\text{ cm}^{-1}$ .<sup>13-19</sup> It is reasonable to expect a similar hydrogen-bonded OH stretch frequency for the AD sites of  $\text{H}^+(\text{MeOH})_n$ . Then, the dominance of the AD sites in large-sized  $\text{H}^+(\text{MeOH})_n$  should result in the convergence of the hydrogen-bonded OH bands to  $3300\text{ cm}^{-1}$ . This is consistent with the observed IR spectral feature of  $n > \sim 10$ .

## Summary

We carried out IR spectroscopy of protonated methanol clusters in the size range from  $n = 4$  up to  $n = 15$ , and their OH stretching vibrations were observed. The free OH stretch band disappeared at  $n = 7$ , and only hydrogen-bonded OH stretches were observed at  $n \geq 7$ . The hydrogen-bonded OH bands converged on a broad band around  $3300\text{ cm}^{-1}$  at  $n \geq \sim 10$ , which is very similar to those observed in neutral cyclic methanol clusters. A simple consideration of the hydrogen bond structure of protonated methanol clusters predicted a bicyclic network structure. The disappearance of the free OH stretch indicates that the bicyclic structure formation is completed at  $n$

$= 7$ , and quantum chemical calculations qualitatively supported this analysis. The convergence of the hydrogen-bonded OH stretch into the  $3300\text{ cm}^{-1}$  band is consistent with the predominance of the two-coordinated (AD) sites in the large-sized clusters of the bicyclic structure.

**Acknowledgment.** We thank Prof. T. Ebata, Prof. H. Ishikawa, and Dr. T. Maeyama for their helpful discussion.

**Supporting Information Available:** Comparison between the infrared spectra of  $\text{H}^+(\text{MeOH})_n$  ( $n = 11-14$ ) by monitoring the  $n - 1$  and  $n - 2$  fragment channels (PDF). This material is available free of charge via the Internet at <http://pubs.acs.org>.

## References and Notes

- (1) Jeffrey, G. A. *An Introduction to Hydrogen Bonding*; Oxford University Press: New York, 1997.
- (2) Zwier, T. S. *Annu. Rev. Phys. Chem.* **1996**, *47*, 205.
- (3) Ebata, T.; Fujii, A.; Mikami, N. *Int. Rev. Phys. Chem.* **1998**, *17*, 331.
- (4) Brutschy, B. *Chem. Rev.* **2000**, *100*, 3891.
- (5) Scheiner, S. *Hydrogen Bonding: A Theoretical Perspective*; Oxford University Press: New York, 1997.
- (6) Kim, K. S.; Tarakeswar, P.; Lee, J. Y. *Chem. Rev.* **2000**, *100*, 4145.
- (7) Miyazaki, M.; Fujii, A.; Ebata, T.; Mikami, N. *Science* **2004**, *304*, 1134.
- (8) Shin, J.-W.; Hammer, N. I.; Diken, E. G.; Johnson, M. A.; Walters, R. S.; Jaeger, T. D.; Duncan, M. A.; Christie, R. A.; Jordan, K. D. *Science* **2004**, *304*, 1137.
- (9) Wu, C.-C.; Lin, C.-K.; Lee, Y. T.; Chang, H.-C.; Jiang, J.-C.; Kuo, J.-L.; Klein, M. L. *J. Am. Chem. Soc.*, submitted for publication.
- (10) Searcy, J. Q.; Fenn, J. B. *J. Chem. Phys.* **1974**, *61*, 5282.
- (11) Wei, S.; Shi, Z.; Castleman, A. W., Jr. *J. Chem. Phys.* **1991**, *94*, 3268.
- (12) Steinbach, C.; Andersson, P.; Kazimirski, J. K.; Buck, U.; Buch, V.; Beu, T. A. *J. Phys. Chem. A* **2004**, *108*, 6165.
- (13) Huisken, F.; Kulcke, A.; Laush, C.; Lisy, J. M. *J. Chem. Phys.* **1991**, *95*, 3924.
- (14) Huisken, F.; Kaloudis, M.; Koch, M.; Werhahn, O. *J. Chem. Phys.* **1996**, *105*, 8965.
- (15) Buck, U.; Schmidt, B. *J. Chem. Phys.* **1993**, *98*, 9410.
- (16) Buck, U.; Ettischer, I. *J. Chem. Phys.* **1998**, *108*, 33.
- (17) Buck, U.; Huisken, F. *Chem. Rev.* **2000**, *100*, 3863.
- (18) Pribble, R. N.; Hagemester, F. C.; Zwier, T. S. *J. Chem. Phys.* **1997**, *106*, 2145.
- (19) Hagemester, F. C.; Gruenloh, C. J.; Zwier, T. S. *J. Phys. Chem. A* **1998**, *102*, 82.
- (20) Narten, A. H.; Habenschuss, A. *J. Chem. Phys.* **1984**, *80*, 3387.
- (21) Chang, H.-C.; Jiang, J.-C.; Lin, S. H.; Lee, Y. T.; Chang, H.-C. *J. Phys. Chem. A* **1999**, *103*, 2941.
- (22) Chang, H.-C.; Jiang, J.-C.; Chang, H.-C.; Wang, L. R.; Lee, Y. T. *Isr. J. Chem.* **1999**, *39*, 231.
- (23) Zang, X.; Yang, X.; Castleman, A. W., Jr. *Chem. Phys. Lett.* **1991**, *185*, 298.
- (24) Miyazaki, M.; Fujii, A.; Ebata, T.; Mikami, N. *Phys. Chem. Chem. Phys.* **2003**, *5*, 1137.
- (25) Herzberg, G. *Molecular Spectra and Molecular Structure II. Infrared and Raman Spectra of Polyatomic Molecules*; Van Nostrand Reinhold Co.: New York, 1945.
- (26) Frisch, M. J.; Trucks, G. W.; Schlegel, H. B.; Scuseria, G. E.; Robb, J. M. A.; Cheeseman, R.; Zakrzewski, V. G.; Montgomery, J. A., Jr.; Stratmann, R. E.; Burant, J. C.; Dapprich, S.; Millam, J. M.; Daniels, A. D.; Kudin, K. N.; Strain, M. C.; Farkas, O.; Tomasi, J.; Barone, V.; Cossi, M.; Cammi, R.; Mennucci, B.; Pomelli, C.; Adamo, C.; Clifford, S.; Ochterski, J.; Petersson, G. A.; Ayala, P. Y.; Cui, Q.; Morokuma, K.; Malick, D. K.; Rabuck, A. D.; Raghavachari, K.; Foresman, J. B.; Cioslowski, J.; Ortiz, J. V.; Baboul, A. G.; Stefanov, B. B.; Liu, G.; Liashenko, A.; Piskorz, P.; Komaromi, I.; Gomperts, R.; Martin, R. L.; Fox, D. J.; Keith, T.; Al-Laham, M. A.; Peng, C. Y.; Nanayakkara, A.; Gonzalez, C.; Challacombe, M.; Gill, P. M. W.; Johnson, B.; Chen, W.; Wong, M. W.; Andres, J. L.; Gonzalez, C.; Head-Gordon, M.; Replogle, E. S.; and Pople, J. A. *Gaussian 98*, revision A.7; Gaussian, Inc.: Pittsburgh, PA, 1998.
- (27) This calculated structure is visualized by using MOLCAT, version 2.5.2.: Tsutsui, Y.; Wasada, H. *Chem. Lett.* **1995**, 517.